4-12-2024

Assessment of satellite-based water requirements for a drip-irrigated apple orchard in Mediterranean agroclimatic conditions

Daniel de la Fuente-Saiz

Samuel Ortega-Farias

Marcos Carrasco-Benavides

Samuel Ortega-Salazar

Fei Tian

See next page for additional authors

Authors

Daniel de la Fuente-Saiz, Samuel Ortega-Farias, Marcos Carrasco-Benavides, Samuel Ortega-Salazar, Fei Tian, Sufen Wang, and Yi Liu

Heliyon 10 (2024) e29688

Contents lists available at ScienceDirect

Heliyon

journal homepage: www.cell.com/heliyon

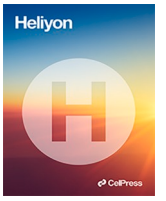

Research article

Assessment of satellite-based water requirements for a drip-irrigated apple orchard in Mediterranean agroclimatic conditions

Daniel de la Fuente-Saiz [a], Samuel Ortega-Farias [a,*], Marcos Carrasco-Benavides [b], Samuel Ortega-Salazar [c], Fei Tian [d,e], Sufen Wang [d,e], Yi Liu [d,e]

[a] Research and Extension Center for Irrigation and Agroclimatology (CITRA) and Research Program on Adaptation of Agriculture to Climate Change (PIEI A2C2), Universidad de Talca, Campus Lircay, Chile
[b] Department of Agricultural Sciences, Universidad Católica del Maule, Curicó, Chile
[c] Department of Civil and Environmental Engineering and School of Natural Resources, University of Nebraska-Lincoln, Lincoln, NE, USA
[d] Center for Agricultural Water Research in China, China Agricultural University, Beijing 100083, China
[e] National Field Scientific Observation and Research Station on Efficient Water Use of Oasis Agriculture in Wuwei of Gansu Province, Wuwei 733000, China

ARTICLE INFO

Keywords:
Energy balance
Evapotranspiration
Crop coefficient
Remote sensing

ABSTRACT

Accurate assessment of evapotranspiration (ETa) and crop coefficient (Kc) is crucial for optimizing irrigation practices in water-scarce regions. While satellite-based surface energy balance models offer a promising solution, their application to sparse canopies like apple orchards requires specific validation. This study investigated the spatial and temporal dynamics of ETa and Kc in a drip-irrigated 'Pink Lady' apple orchard under Mediterranean conditions over three growing seasons (2012/13, 2013/14, 2014/15). The METRIC model, incorporating calibrated sub-models for leaf area index (LAI), surface roughness (Z_{om}), and soil heat flux (G), was employed to estimate ETa and Kc. These estimates were validated against field-scale Eddy Covariance data. Results indicated that METRIC overpredicted Kc and ETa with errors less than 10 %. These findings highlight the potential of the calibrated METRIC model as a valuable decision-making tool for irrigation management in apple orchards.

1. Introduction

Apple trees (*Malus domestica* Borkh) are a major fruit crop grown under irrigation in Mediterranean and semi-arid regions, with an annual global production of around 87 million tons [1,2]. However, the future of apple production is threatened by water scarcity, which directly reduces the availability of water for irrigation and compromise the sustainability of crop water resources [3,4]. Global warming characterized by rising temperatures and water scarcity [5–7], poses a serious challenge to apple orchards by increasing their water requirements (ETa). Drought stress significantly affects apple tree metabolism, adversely affecting fruit quality and size [1]. Hence, developing appropriate irrigation schedules emerges as a critical strategy for adapting apple production to the effects of climate change, where accurately estimating the ETa is a key factor in this regard [8,9].

The daily ETa is calculated by multiplying the single crop coefficient (Kc) for each specific growth stage (initial, middle, and end) by

* Corresponding author.
E-mail address: sortega@utalca.cl (S. Ortega-Farias).

https://doi.org/10.1016/j.heliyon.2024.e29688
Received 13 March 2024; Received in revised form 2 April 2024; Accepted 12 April 2024
Available online 16 April 2024

the reference evapotranspiration (ETo) obtained using the FAO-56 Penman-Monteith method [10–12]. This method is still widely used to estimate ETo and requires air temperature, relative humidity, wind speed, and solar radiation measurements from a weather station. However, the Kc values obtained from literature are derived from specific experimental conditions, representing average values that may not sufficiently capture the influence of spatial variability at field scale and may not be adequate to use in different crop and climate conditions [13–15]. As a result, extrapolating those Kc values to the entire field (in both time and space) can be challenging for farmers and may lead to inaccurate irrigation scheduling in an operational scenario [11,16,17].

To address this limitation, satellite-based remote sensing approaches have emerged as a cost-effective alternative for estimating and mapping the spatial and temporal variability of both Kc and ETa throughout the growing season [17–20]. The Landsat satellite family provides auxiliary images every 16 days, or every 8 days when used in combination. These images can be combined with public ground weather data and easy to use open-source software for processing satellite algorithms [21–23]. Residual surface energy balance (RSEB) algorithms, such as SEBAL [24], SEBALI [25], METRIC [26], S-SEBI [27], T-SEB [28], among others, have been extensively validated in

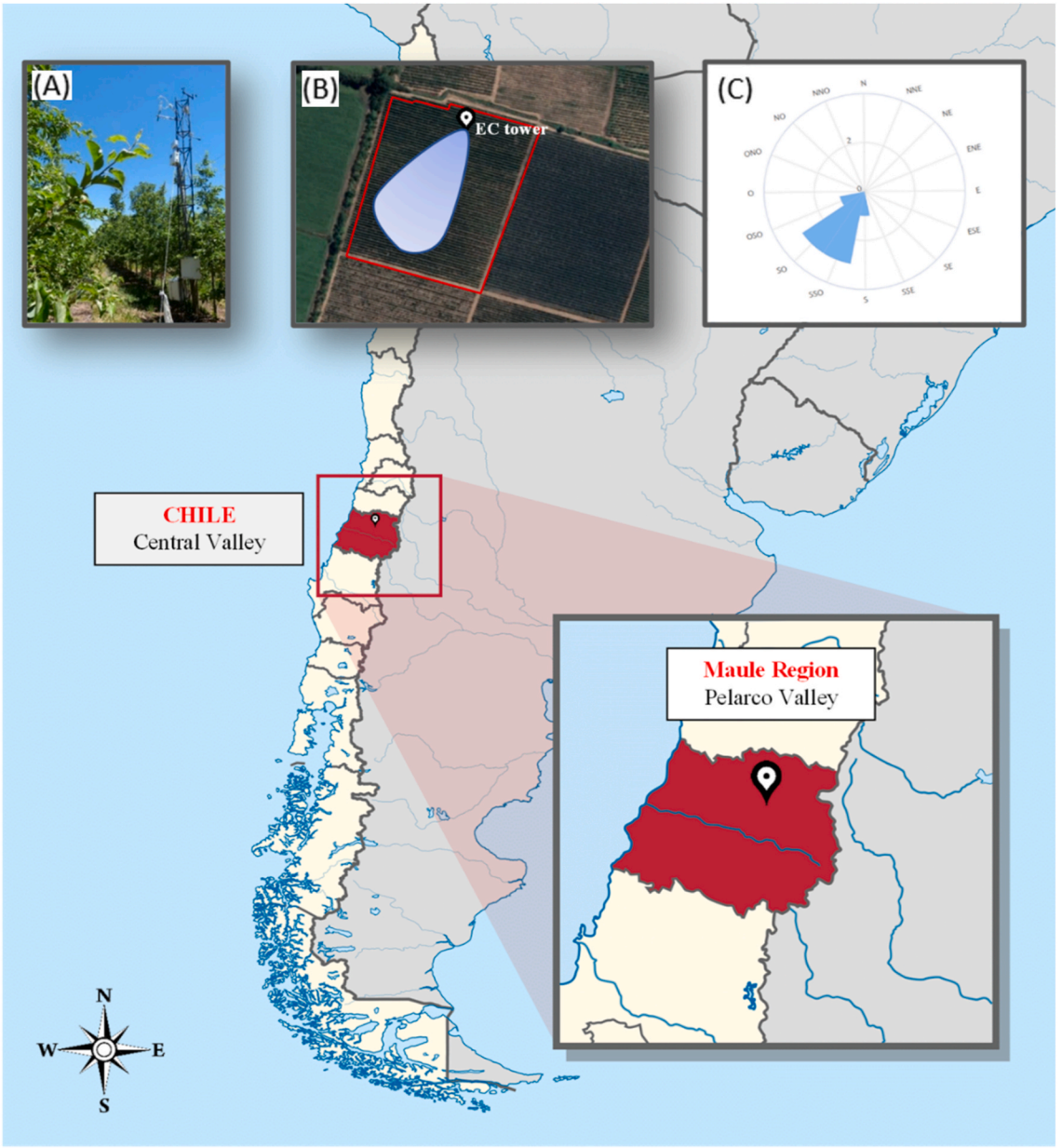

Fig. 1. Reference location of the drip-irrigated apple orchard under study. On the top: (**A**) Apple orchard tree architecture and Eddy Covariance Tower (EC Tower). (**B**) Experimental plot highlighted in a red polygon, EC tower location and Footprint area, (**C**) predominant wind direction on the study site (Pelarco Valley, Maule Region, Chile).

different agricultural areas for irrigation management. While these physically-based models, utilizing the thermal band of satellite imagery, have shown strong agreement with field observations in annual crops [19,29–32], most RSEB algorithms requires adaptation for non-homogeneous crops with diverse canopy architectures [33–36]. Therefore, calibration and subsequent validation are necessary for their application in these scenarios.

Sparse woody crops, like apple orchards, pose a challenge for accurate and representative Kc calculation due to their complex three-dimensional structure. From a satellite's perspective, a fruit orchard consists of distinct rows of trees interspersed with bare soil [34,37]. This spatial arrangement influences the partitioning of net radiation (Rn) into soil heat flux (G), latent heat flux (LE), and sensible heat flux (H) within the orchard. Consequently, it impacts the spatial variability of Kc and ultimately, ETa [38]. Several factors can further influence this spatial variability, including soil type, climate, tree age, cultivar, orchard orientation, tree height and spacing, canopy architecture, and the training system employed [11,12]. By capturing these influences, satellite data provides a comprehensive view of the actual water conditions within the orchard.

The METRIC model has been successfully adapted for sparse woody crops, including vineyards and fruit orchards, by several researchers. In this regard [32,39], reported that the model incorporating calibrated functions of leaf area index (LAI), surface roughness (Z_{om}), and G achieved an accuracy of approximately 11 % in estimating Kc for a drip-irrigated vineyard. For a drip-irrigated olive orchard, [40] indicated that the METRIC model using calibrated functions of LAI, $Z_{om,}$ and G underestimated the Kc and ETa by less than 4 % and 6 %, respectively. Ref. [34] found that adjusted METRIC algorithms of LAI, $Z_{om,}$ and surface temperature for estimating ETa in a super-intensive olive orchard had a mean bias of 12.6 %. Ref. [41] also found that METRIC, when applied with corrections in the Z_{om} sub-model, produced an RMSE of 0.045 and 0.25 mm/day for Kc and ETa, respectively, in an olive orchard. For a drip-irrigated apple orchard, [33] indicated that METRIC using calibrated sub-models improved the estimation of LE and H fluxes with errors of +5 % and +16 %, respectively. However, the uncalibrated METRIC functions resulted in higher errors of +29 % for H and +26 % for LE. Supporting these findings, [42] considers this level of accuracy sufficient for irrigation management purposes based on satellite monitoring.

Inaccuracies in satellite-based estimations of Kc and ETa can have significant negative consequences for farmers, water managers, and the long-term sustainability of water resources in the orchard. This is particularly critical in Mediterranean fruit-growing regions, where apple orchards often face water scarcity [44,45]. Precise Kc and ETa data are essential for effective irrigation management, and satellite-based remote sensing technology, exemplified by the calibrated METRIC model, offers a promising solution.

Remote sensing technology has been suggested as a decision-making tool to improve irrigation scheduling in drip-irrigated apple orchards growing under Mediterranean agroclimatic conditions [42]. However, the ability of the calibrated METRIC model to capture the unique spatial and temporal variability of Kc and ETa within apple orchards remains unverified. This study aims to address this gap by evaluate the spatial and temporal dynamics of Kc and ETa for a drip-irrigated apple orchard using the METRIC model with calibrated functions LAI, Z_{om}, and G.

Table 1
Values of cumulative growing degree days (base 10) (CGDD) associated with the BBCH-scale for the main phenological stages of the drip-irrigated apple orchard (Pelarco Valley, Maule Region, Chile).

Growing Season	Date (dd-mm-yyyy)	Day of year (DOY)	CGDD (°C)	BBCH Index
2012/13	27-09-2012	271	35.7	57
	17-10-2012	291	72.7	61
	31-10-2012	305	111.6	71
	26-11-2012	331	270.6	74
	12-02-2013	43	970.2	77
	15-03-2013	74	1175.5	81
	16-04-2013	106	1297.3	87
2013/14	10-09-2013	253	37.2	57
	14-10-2013	287	72.2	61
	24-10-2013	297	110.8	71
	24-11-2013	328	271.1	74
	06-02-2014	37	969.4	77
	03-03-2014	62	1178.6	81
	20-03-2014	79	1295.7	87
2014/15	21-09-2014	233	37.7	57
	14-10-2014	287	72.1	61
	25-10-2014	298	112.1	71
	23-11-2014	327	267.4	74
	08-02-2015	39	970.1	77
	04-03-2015	63	1171.3	81
	19-03-2015	78	1305.0	87

BBCH-scale: **57** = Pink bud stage: flower petals elongating; sepals slightly open; petals just visible; **61** = Beginning of flowering: about 10 % of flowers open; **71** = Fruit size up to 10 mm; **74** = Fruit diameter up to 40 mm; Fruit erect; **77** = Fruit about 70 % final size; **81** = Beginning of ripening: first appearance of cultivar-specific color; and **87** = Fruit ripe for picking. BBCH = *Biologische Bundesanstalt, Bundessortenamt and CHemical industry*.

2. Materials and methods

2.1. Site description

The experiment was conducted during three consecutive growing seasons (2012/13, 2013/14, and 2014/15) in a drip-irrigated apple (*Malus domestica* 'Pink Lady') orchard planted in 2008 on 'M7' rootstock. The study site was 5.5 ha (ha) plot located in the Pelarco Valley, Maule Region, Chile (35°25.2′ S; 71°23.6′ W; 189 m.a.s.l.) and surrounded by other apple orchards with the same agronomic management (Fig. 1). Apple trees were trained under the vertical axis system and fruit thinning was carried out every season to obtain a crop load between 200 and 250 fruits per tree. The planting framework is a high-density system with a spacing of 1.5 × 4.0 m (1667 trees/ha). The average tree height was 4.0 ± 0.07 m, canopy width 1.55 ± 0.02 m, and mean rooting depth of 0.8 ± 0.15 m measured directly by root pit excavations. During this study, the orchard was irrigated using two 4.0 l/h surface drippers per tree (precipitation rate = 5.33 mm/h) and maintained under non-water stress conditions. The experimental site has a Mediterranean climate, with an annual rainfall of 690 mm, most of which (75 %) occurs during the winter months (May to October) [6,46]. The soil is loamy clay with a flat topography (34 % clay, 30 % silt, and 36 % sand).

2.2. Apple phenological stages and water status

Field data were collected from 18 spatially distributed sentinel trees over three growing seasons, from mid-November to late March. The apple phenological stages were classified using the BBCH-scale (*Biologische Bundesanstalt, Bundessortenamt and CHemical industry*) for pome fruit [47], which was associated with the Cumulative Growing Degree Days (CGDD) base 10. Based on visual inspection, the main phenological stages were identified as follows: (57) = Pink bud stage: flower petals elongating; sepals slightly open; petals just visible; (61) = Beginning of flowering: about 10 % of flowers open; (71) = Fruit size up to 10 mm; fruit fall after flowering; (75) = Fruit about half final size; (77) = Fruit about 70 % final size; (81) = Beginning of ripening: first appearance of cultivar-specific color; and (87) = Fruit ripe for picking. The starting stage was assumed when almost 50 % of apple trees had reached a new phenological state (Table 1).

The midday stem water potential (Ψx) was measured with a pressure chamber (PMS 600, PMS Instrument Company, Corvallis, OR., USA) to evaluate the water status of the experimental plot. The measurements were performed at solar noon over 36 fully expanded leaves (two per tree; 18 sentinel trees) on both sides of the apple rows. Leaves were encased in a plastic bag and wrapped in aluminum foil at least 2 h before measurement [48].

2.3. Weather data for ETo estimation

To estimate daily evapotranspiration of apple trees using the METRIC model, a reference automatic weather station (AWS) installed over a well-watered (grass or alfalfa) surface is needed in the process [26,49]. For this purpose, a grass reference AWS (Adcon Telemetry model A733, add wave) was installed 1000 m East from the experimental site (35°25,1′S; 71°23,1′W, 180 m.a.s.l.). Weather measurements include solar radiation, air temperature, relative humidity, wind speed and direction, and precipitations. Monthly maintenance was carried out on the AWS's sensors and over the grass reference surface to control growth, as [10] suggested. Instantaneous (ETo_{inst}; mm/h) and daily ETo (mm/day) were computed using the pyfao56 module in python [50] based on the FAO-56 Penman-Monteith method [10].

2.4. Field measurements of Kc and ETa

Apple Kc and ETa were obtained using the surface energy balance (SEB) technique based on field measurements of net radiation (Rn), soil heat flux (G), latent heat flux (LE), and sensible heat flux (H), and the AWS data. Fluxes of Rn were measured every half-minute by a four-way net radiometer (CNR4, Kipp and Zonen Inc., Delft, The Netherlands) installed on a tower of 5.5 m high located inside the orchard. Fluxes of LE and H were measured ten times per second (10 Hz frequency) by a three-dimensional sonic anemometer (CSAT-3, Campbell Scientific Inc., Logan, UT, USA) and an infrared gas analyzer (LI-7500, LI-COR Inc., Lincoln, NE, USA), respectively. To obtain measurements in the footprint area from the EC system, the CSAT-3 and LI-7500 instruments were installed considering the predominant wind direction (south-west; S-W, 270°). The fetch information (source area for turbulent fluxes calculation) was obtained by EC fluxes following [51]. The footprint model analysis showed that the peak footprint location (x_{max}) was obtained at 15 m. A cumulative normalized contribution to the flux measurement (CNF) of 90 % was obtained at 278 m (1:46 ratio), which is similar to other field observations reporting fetch ranging from 1:15 to 1:75 [52,53]. Measurement was recorded in a CR5000 datalogger (Campbell Scientific Inc., Logan, UT, USA). To close the surface energy balance, the hourly LE values from the EC system were recalculated using the Bowen ratio approach [54].

For soil energy fluxes calculation, four soil heat flux plates and four soil thermocouples were installed in the ground under tree rows, and four others were located between rows to estimate G fluxes of the orchard [38]. This installation allows us to consider the effect of the shadow between rows during the day. Soil heat flux plates (HFT3, Campbell Scientific Inc., Logan, UT, USA) were buried at a depth of 0.08 m, and thermocouples (TCAV, Campbell Scientific Inc., Logan, UT, USA) were positioned at 0.02 and 0.06 m depth above each heat flux plate [55]. Measurement was recorded using a CR3000 datalogger (Campbell Scientific Inc., Logan, UT, USA) installed at the bottom of the tower at half-hour time intervals.

The statistical analyses of the hourly energy balance closure from the EC system indicated that the turbulent fluxes (H + LE) were

14 % lower than the total available energy (Rn – G) in the apple orchard footprint. A linear regression through the origin indicated that the coefficient of determination (R^2) was 0.87 for days with available satellite images. These results agreed with similar studies that use micrometeorological information based on drip-irrigated sparse crops such as vineyards and olives trees [32,33,38,56]. Also, results indicated that the data was appropriate for accurate estimations of Kc and ETa over the apple orchard using the EC system in the footprint area. The statistical methods, flux recalculations, and theoretical foundations used in this study to estimate SEB fluxes from EC system data are extensively detailed by Ref. [57].

2.5. Remote sensing data

For the computation of time series Kc and ETa using the METRIC model, a dataset of 20 Landsat 7 ETM + satellite images (Table 2) were downloaded from the USGS Geospatial Data Source repository (www.usgs.gov) for the three growing seasons. Satellite images were selected based on a cloud cover criterion of less than 30 % over the study area. The images were downloaded with a default standard terrain correction (Level 1T). However, satellite images for September and April were not available due to the heavy cloud cover in the apple orchard (Table 2). Nevertheless, the Landsat 7 ETM + images used in this study (Path 233/Row 85) did not have any pixel gaps.

The original METRIC model proposed by Ref. [26] and its modification for apple trees proposed by Ref. [33] were used in this study to calculate and map daily single Kc and ETa on the satellite dataset using the Water package in R [21]. Model modifications were related to the parameterization in the sub-models of LAI, Z_{om}, and G fluxes for apple orchards. These calibrated sub-models, including their statistical performance obtained in this study, are presented in detail in Table 3.

After incorporating these sub-models in the process, the METRIC model computes pixel by pixel LE in the orchard based on the remotely sensed energy balance derived from Landsat satellite imagery. Thus, LE is obtained as a residual of the surface energy balance method (Eq. (1)).

$$LE = Rn - G - H \tag{1}$$

where, LE is the latent heat flux (W/m^2), Rn is the net radiation from the sun, atmosphere, and surface (W/m^2), G is the soil heat flux into the ground (W/m^2), and H is the sensible heat flux to the air (W/m^2).

Following the computation of all components in Equation (1), instantaneous evapotranspiration (ETa_{inst}) at the time of satellite overpass (expressed in mm/h) is determined at the pixel level (Eq. (2)). This calculation involves dividing the LE derived from Equation (1) by both the latent heat of vaporization (λ, J/kg) and the water density (ρw = 1000 kg/m^3).

$$ETa_{inst} = 3600 \bullet \frac{LE}{\lambda \bullet \rho w} \tag{2}$$

Then, the Kc (also called reference evapotranspiration fraction; ETrF) was calculated as the ratio between instantaneous ETa (ETa_{inst}) at pixel level and the instantaneous ETo (ETo_{inst}), obtained from the local weather station at the image acquisition time (Eq. (3)).

$$ETrF = Kc = \frac{ETa_{inst}}{ETo_{inst}} \tag{3}$$

Finally, daily values of ETa (mm/day) were calculated for each pixel based on daily ETo as follows (Eq. (4)):

$$ETa = Kc * ETo \tag{4}$$

where, Kc is the pixel level satellite-based crop coefficient (or ETrF) and ETo is the daily reference evapotranspiration (mm/day) computed from the weather station.

During the post-processing of each available satellite image, an area of interest was selected, which was a 30-m perimeter from the inward edges of the experimental plot using the QGIS (Quantum GIS) 3.28.10 open-source software. This procedure excludes any contamination by pixels that fell outside the study site, such as internal orchard roads and surrounding apple plots [32]. Results from the calibrated METRIC model were compared with field measurements using the EC system data (Fig. 1A).

Table 2
Summary of Landsat 7 ETM + satellite imagery used to estimate Kc over the apple orchard (path 233/row 85) (Pelarco Valley, Maule Region, Chile).

Season 2012/13		Season 2013/14		Season 2014/15	
Date (dd-mm-yy)	Day of Year (DOY)	Date (dd-mm-yy)	Day of Year (DOY)	Date (dd-mm-yy)	Day of Year (DOY)
11-11-2012	316	30-11-2013	334	01-11-2014	305
27-11-2012	332	16-12-2013	350	17-11-2014	321
29-12-2012	364	17-01-2014	17	04-01-2015	4
30-01-2013	30	02-02-2014	33	05-02-2015	36
15-02-2013	46	18-02-2014	49	21-02-2015	52
03-03-2013	62	06-03-2014	65	09-03-2015	68
19-03-2013	78	22-03-2014	81	–	–

Satellite images for September and April were unavailable due to the high cloud cover in the study area.

Table 3
List of calibrated functions of the METRIC model considered in the study, including their equations and statistics summary on apple orchards [33].

Sub-Model	Formula	Statistics
LAI	$2.42 - 1.04e^{-502.1 \bullet NDVI^{9.32}}$	$R^2 = 0.98$ RMSE = 0.2 m^2/m^{-2} MAE = 0.15 m^2/m^{-2} d = 0.44
Z_{om}	$\left(\left(1 - \exp\left(\frac{-0.06 \bullet LAI}{2}\right)\right) \bullet exp\left(\frac{-0.06 \bullet LAI}{2}\right)\right) \bullet h$	$R^2 = 0.94$ RMSE = 0.03 m MAE = 0.03 m d = 0.91
G	$Ts(0.00261 \bullet 0.06 + 0010) \bullet (1 - 0.98 \bullet NDVI^4) \bullet Rn$	$R^2 = 0.97$ RMSE = 16 W/m^2 MAE = 14 W/m^2 d = 0.84

LAI = Leaf Area Index; Z_{om} = momentum roughness length (m); G = soil heat flux (W/m^2); h = canopy height (m); NDVI = normalized difference vegetation index; Rn = net radiation (W/m^2); Ts = radiometric surface temperature from Landsat TIR Band (°C); RMSE = root mean square error; MAE = mean absolute error; d = index of agreement.

2.6. Data analysis

Instantaneous and daily Kc and ETa values computed by the METRIC model were compared to the values directly measured in the footprint area of the EC system. This footprint area was estimated as 4170 m^2 in the S-W wind direction departing from the EC tower placement (Fig. 1B, C). The pixel-by-pixel comparison was made considering an average of 90 × 90 m^2 area (3 × 3 pixels), agreeing with the Landsat pixels resolution (30 × 30 m). Measured values of Kc and ETa from the EC system (Kc_{eddy} and ETa_{eddy}) were compared with the original and calibrated estimations of the METRIC model (Kc_{metric} and ETa_{metric}). Only data of 2012/13 growing season (validation set) was use in this step. A regression analysis was conducted to evaluate the agreement between observed and estimated values, represented by coefficient (*b*).

A series of statistical tests, as described by Refs. [58,59], were used to evaluate the statistical differences among variables at the 95 % confidence level. These statistics include the *t*-test (for *b*), root mean square error (RMSE), mean absolute error (MAE), and the index of agreement (*d*).

It is important to note that only the validation sets were used in the statistical analysis. The calibration sets (2013/14 and 2014/15) were deliberately excluded to avoid any potential bias or over-corrections in the results.

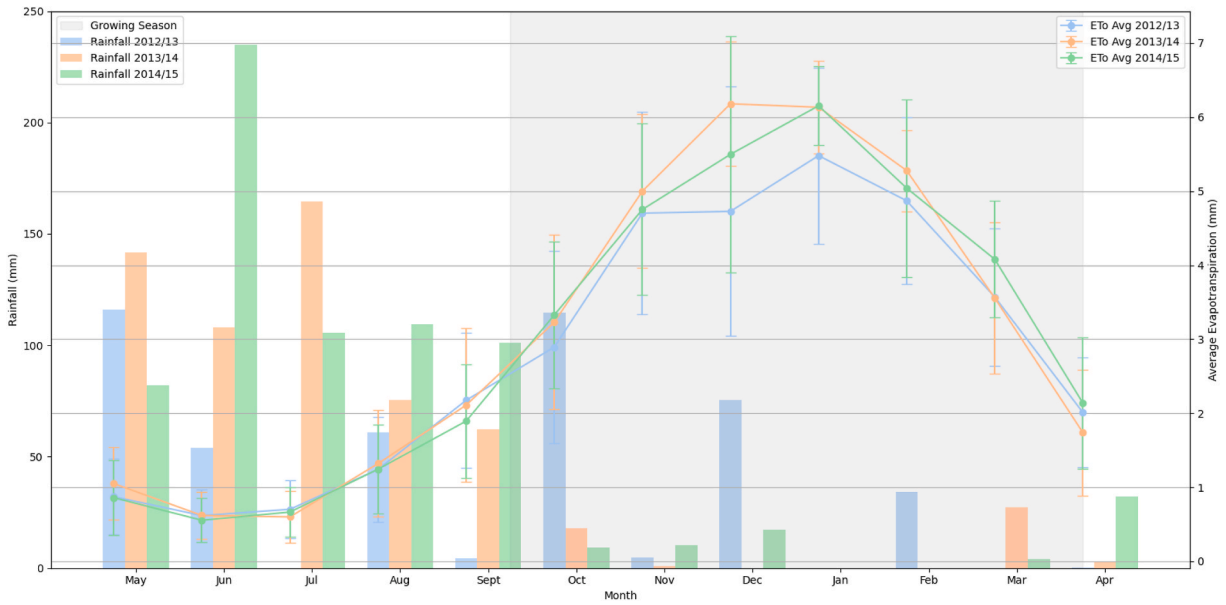

Fig. 2. Monthly values of rainfall and accumulative grass reference evapotranspiration (Penman–Monteith FAO-56 ETo) during the 2012/13, 2013/14, and 2014/15 seasons (Pelarco Valley, Maule Region, Chile). The gray shadow area corresponds to apple orchard growing season.

3. Results

3.1. Weather conditions and apple tree's water status

The meteorological conditions across the growing seasons were consistent, characterized by dry and hot climates with reduced rainfall events from September through April (Fig. 2). In general, annual values of ETo during apples tree's growing season (from September to April in Chile, Table 1) were 919 mm, 1005 mm, and 995 mm. The highest daily ETo was recorded in summer (mid-December to February) with 6.1 ± 0.9 mm/day. The annual rainfall for the 2012/13, 2013/14, and 2014/15 growing seasons was 233.6 mm, 111.0 mm, and 174.2 mm, respectively (Fig. 2). Rainfall events were concentrated from May to mid-September, with minimal rain events into spring and summer (Fig. 2). Consequently, minimal rainwater was stored in the soil profile for orchard use throughout these seasons. The daily air temperature for the apple trees' growing period was characterized by cold conditions at the beginning of the spring, presenting some events of night frost until mid-October. Then, the climate changed to dry and hot weather conditions during the mid-summer, showing daily maxima above 35 °C (Table 4). The average maximum vapor pressure deficit (VPD) values were 1.28 ± 0.31 kPa for all evaluated growing seasons (Table 4). From mid-November to late March, these dry and hot atmospheric conditions presented sunny days, occasionally cloudy, and no considerable rainfall periods (Fig. 2). In this regard, the cumulative rainfall and evapotranspiration were similar for all three growing seasons. However, the cumulative reference evapotranspiration (water loss) was greater than the cumulative rainfall (water input), suggesting that supplementary irrigation was necessary from November onwards for all three study periods. The total cumulative irrigation volume for the three growing seasons was 414 mm/ha, 465 mm/ha, and 436 mm/ha, respectively.

3.2. Comparison between satellite-based Kc against EC measurements

Fig. 3 shows a comparison of the single-Kc and ETa values computed from the Eddy covariance (EC) system (Kc_{eddy} and ETa_{eddy}) and those computed from the METRIC model using the standard and calibrated functions of LAI, Z_{om}, and G for apple trees (Kc_{metric} and ETa_{metric}). The computed values from the METRIC using the original sub-models (green triangles) resulted in points above the 1:1 line for both Kc_{metric} and ETa_{metric} values. On the other hand, using the calibrated sub-models of LAI, Z_{om} and G significantly improved these trends in the daily Kc_{metric} and ETa_{metric} estimations (blue circles), which moved closer to the 1:1 line. The statistical analysis showed that the standard METRIC model had a MAE and RMSE of 0.18 and 0.19, respectively, for Kc estimations, while the METRIC using the calibrated sub-models had a MAE and RMSE of 0.04 and 0.07, respectively (Table 5). The *t*-test of the ratio of Kc_{eddy} to Kc_{metric} was statistically significant at the 95 % confidence level, indicating that the calibrated functions for apple trees (LAI, Z_{om}, and G) reduced the overestimation of Kc_{metric} with an error of 10 %. The improvements in the estimation of Kc were also reflected in the daily estimations of ETa_{metric} in the apple orchard. The statistical analysis showed that the calibrated sub-algorithms of the METRIC

Table 4
Summary of meteorological conditions during the studied apple tree growing seasons (Pelarco Valley, Chile).

Growing Season		Max Temp. (°C)	Min. Temp. (°C)	Average DPV (kPa)
2012/13	Sep	26.2	−0.9	0.2
	Oct	24.5	−0.8	0.3
	Nov	30.3	2.5	0.6
	Dec	31.4	3.5	0.6
	Jan	34.2	7.0	0.7
	Feb	35.5	5.3	0.7
	Mar	30.3	0.9	0.5
	Apr	29.5	−1.8	0.3
Annual value		**30.2**	**2.0**	**0.5**
2013/14	Sep	26.4	−3.3	0.2
	Oct	28.7	−0.4	0.3
	Nov	32.2	3.1	0.6
	Dec	33.1	5.5	0.9
	Jan	36.1	6.4	0.9
	Feb	32.6	3.4	0.7
	Mar	30.5	1.8	0.6
	Apr	24.2	−2.8	0.2
Annual value		**30.5**	**1.7**	**0.6**
2014/15	Sep	21.8	−0.5	0.2
	Oct	28.4	−1.7	0.4
	Nov	31.7	0.7	0.6
	Dec	33.1	4.5	0.7
	Jan	35.0	6.1	0.9
	Feb	33.4	4.0	0.8
	Mar	34.1	3.0	0.7
	Apr	28.2	−0.8	0.3
Annual value		**30.7**	**1.9**	**0.6**

Max. Temp. = maximum air temperature; Min. Temp. = minimum air temperature; Average VPD = Average vapor pressure deficit.

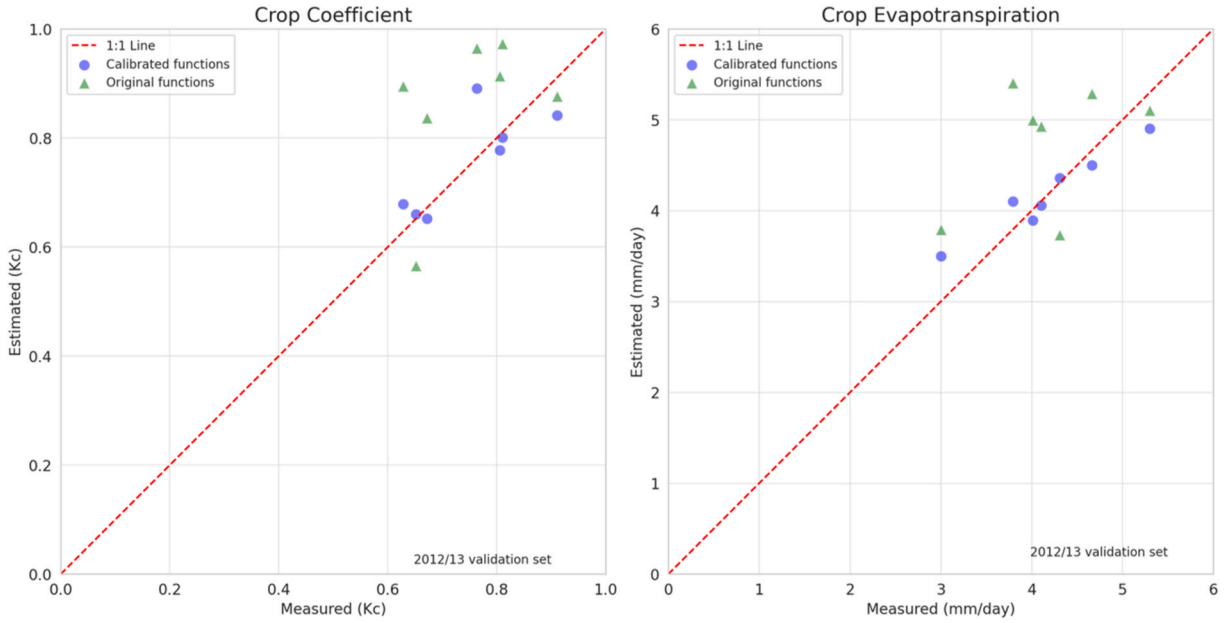

Fig. 3. Comparison between observed and estimated values of Crop Coefficient (Kc) and actual evapotranspiration (ETa) of the drip-irrigated apple orchard for validation season (Pelarco Valley, Maule Region, Chile). Green triangles and blue circles corresponded to the METRIC simulations with the original and calibrated sub-models of leaf area index (LAI), momentum roughness length (Z_{om}), and soil heat flux (G), respectively.

Table 5
Statistical analysis of measured crop coefficient (Kc) and daily actual evapotranspiration (ETa) versus estimated values using the original and calibrated METRIC model for a high-density apple orchard (Pelarco Valley, Maule Region, Chile, Validation set = 2012/13 growing season).

Variable	With Original METRIC sub-models	With Calibrated METRIC sub-models
Kc_{eddy} vs Kc_{metric}		
RMSE	0.18	0.07
MAE	0.19	0.04
b	1.18	1.10
d	0.54	0.84
t-test	F	F
ETa_{eddy} vs ETa_{metric}		
RMSE	1.03 (mm/day)	0.42 (mm/day)
MAE	0.96 (mm/day)	0.29 (mm/day)
b	1.17	1.07
d	0.48	0.93
t-test	F	F

RMSE = root mean square error; MAE = mean absolute error; d = index of agreement; b = slope between estimated/observed T = true hypothesis (b = 1); F = false hypothesis (b ≠ 1). Subscripts: "$_{metric}$" was computed by the METRIC model, "$_{eddy}$" was measured by the Eddy covariance system.

model were able to reduce the biases in daily ETa_{metric} by 7 %, which is equivalent to a 0.29 and 0.42 mm/day in the MAE and RMSE, respectively (Table 5).

3.3. Seasonal evolution of satellite-based Kc

Daily values of Ψx and crop coefficients obtained by the Eddy Covariance system (Kc_{eddy}) and calculated by METRIC model (Kc_{metric}) are indicated in Fig. 4. This Figures indicates that Ψx ranged from −0.9 to −1.49 MPa for the study periods. Also, Fig. 4 shows a comparison of Kc curves for different phenological stages of apple trees. The estimates of remotely sensed Kc were made using the original and calibrated METRIC functions were compared to the standard Kc values suggested in the FAO-56 tables, and the measured Kc from EC system. The satellite-based Kc curve for the 2012/13 growing season spans 165 days, from day of year (DOY) 316 of 2012 (mid-November) to DOY 78 of 2013 (mid-March). This is the growing season validation period defined in Table 2. It is important to note that the cloudiness in the study area, especially from September to October, made it impossible to obtain clear Landsat images of the apple orchard at the beginning of the growing season (Table 2). The METRIC model using calibrated functions of LAI, Z_{om} and G

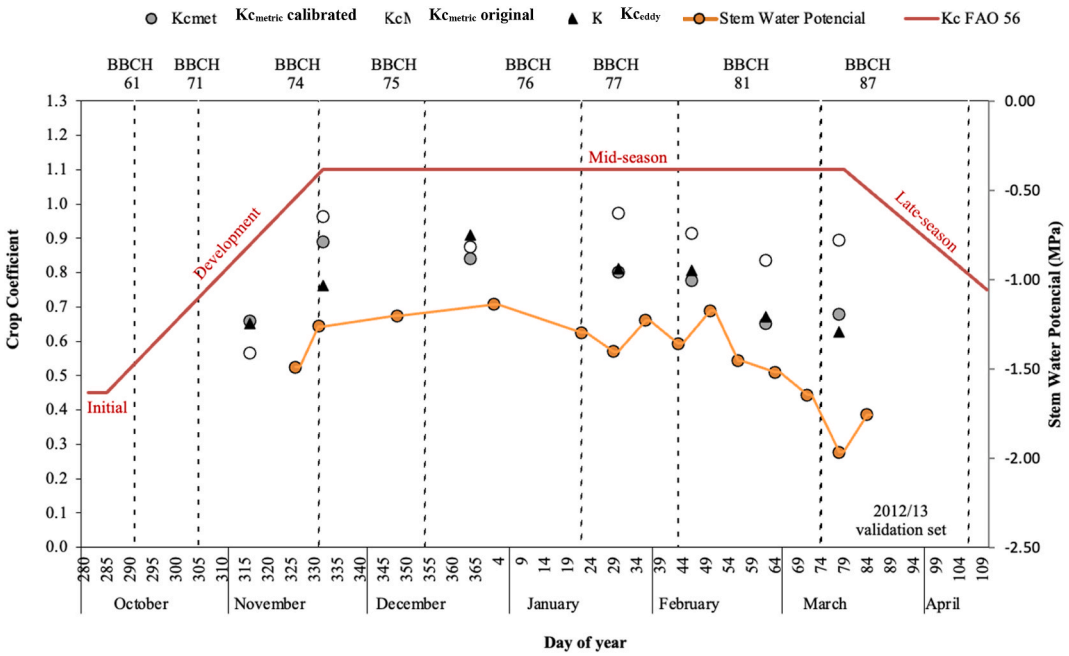

Fig. 4. Daily values of midday stem water potential and crop coefficients obtained by the eddy correlation system (Kc_{eddy}) and calculated by METRIC model (Kc_{metric}) for the main phenological stages of a drip-irrigated apple orchard (Pelarco Valley, Maule Region, Chile). White and dark circles corresponded to original and calibrated sub-models of leaf area index, momentum roughness length, and soil heat flux, respectively. Phenological scales 61, 71, 75, 77, 81 and, 87 correspond to 30 % Flowering, Fruit size 10 mm, Fruit at half size, Fruit at 70 % of final size, Pre-harvest, and Harvest, respectively. BBCH = *Biologische Bundesanstalt, Bundessortenamt and CHemical industry*.

produced Kc values closer to the ones measured using the EC system during the growing season than the standard METRIC version, as shown in Fig. 3 and Table 5. The maximum difference between Kc_{metric} and Kc_{eddy} values was found at BBCH 74 (DOY 332), with a difference of 0.13.

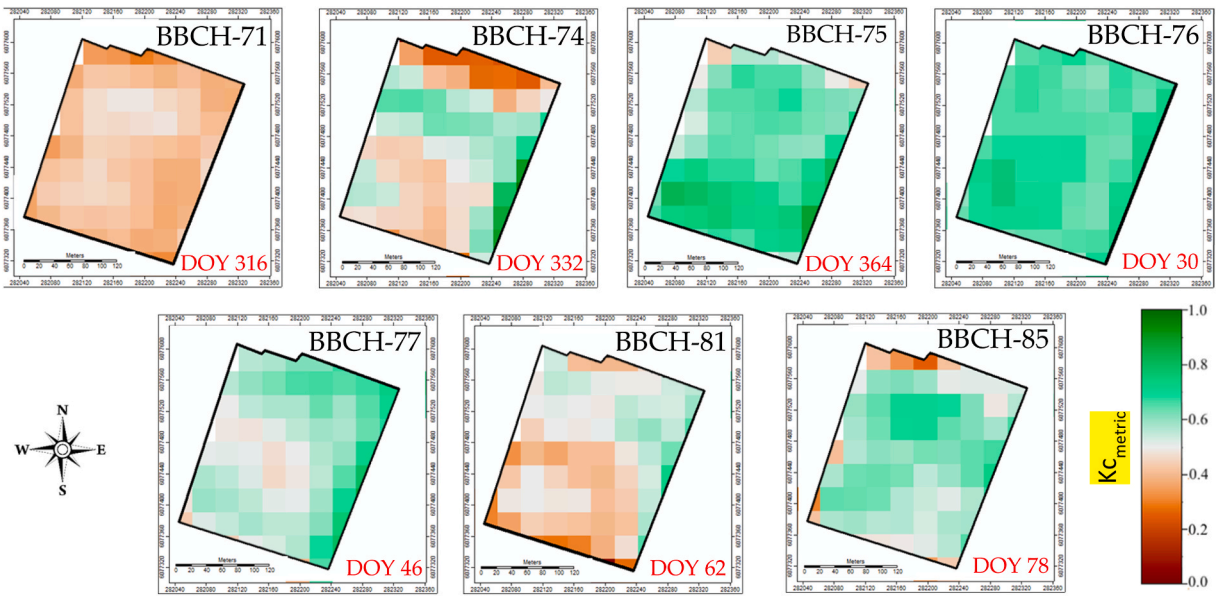

Fig. 5. Spatial and temporal distribution of satellite-based crop coefficient (Kc_{metric}) of a drip-irrigated apple orchard during the 2012/13 growing season computed with the calibrated sub-models of METRIC (Pelarco Valley, Maule Region, Chile). BBCH phenological stages scale: **71** = Fruit size up to 10 mm; fruit fall after flowering; **74** = Fruit diameter up to 40 mm; Fruit erect; **75** = Fruit about half final size; **76** = Fruit about 60 % final size; **77** = Fruit about 70 % final size; **81** = Beginning of ripening; **85** = Pre-harvest, advanced ripening: increase in the intensity of cultivar-specific color. BBCH = *Biologische Bundesanstalt, Bundessortenamt and CHemical industry*.

Fig. 4 shows that the Kc values estimated using the modified METRIC model during the apple trees' growing season (gray circles) were in close agreement with those measured using the EC system (black triangles). On the other hand, the values obtained using the standard METRIC model (white circles) were generally further from the measured values. The main differences between the estimated and measured values of Kc_{metric} were obtained during the apple trees' development and late growth stages (BBCH 76 to BBCH 81) (Fig. 4). Here, the daily Kc computed from the standard METRIC model was 0.93, contrasting with the one obtained from the EC tower ($Kc_{eddy} = 0.73$). Likewise, at the end of the growing season, the differences between measured and computed Kc's using the standard model reached up to 0.27 (DOY 78).

3.4. Spatial patterns of satellite base-Kc

Fig. 5 shows the spatial patterns of Kc maps obtained from the calibrated METRIC model during the main phenological stages of apple trees in the 2012/2013 growing season (validation set). Pixel-based Kc values are classified into color-coded categories from brown to green, across different phenological stages. The brown category indicates lower Kc values (higher water stress), while the green category likely corresponds to higher Kc values (optimal water conditions). The white category represents an intermediate state. These visual groupings of Kc offer a perspective on the spatial variability of Kc during critical growth phases, as indicated by the differing phenological stages labeled BBCH-71 through BBCH-85 and the corresponding days of the year (DOY). The highest Kc_{metric} values were observed in the mid-growing season (from the stages BBCH 74 to 76), when fruits reach between 30 and 60 % of final size. The highest spatial differences of pixel-by-pixels Kc were observed on DOY332, which presented a coefficient of variation (CV) of 18 % in the orchard. In contrast, the lowest spatial variability in Kc was found when apples reached the BBCH-76 growing stage (DOY30) with a CV of 4 %. The observed spatial variability in Kc on DOY 332 was attributed to the presence of a grass cover between tree rows, particularly on the north side of the plot (Fig. 1A). This grass cover emerged following spring rain and the raising air temperatures these days (November) (Fig. 2). In the case of DOY 62, the substantial spatial variability in Kc observed via satellite imagery can be attributed to irregular distribution of water application.

4. Discussion

4.1. Satellite-based Kc and ETa comparison to Eddy covariance field-data

The METRIC model is an operational single-layer model that uses local meteorological data and thermal and multispectral Landsat satellite images to estimate Kc and ETa as a residual of the surface energy balance (RSEB). It was initially developed to produce consistent, pixel-by-pixel maps of the ETa over agricultural lands with full-cover crops of soil [26]. Ref. [17] found that the model can estimate very well the Kc for full-cover crops such as alfalfa, bean, corn, pea, sugar beet, and grain with an average error of 5 %. However, in the case of sparse woody crops, such as apple orchards, the short vegetation coverage in the soil between tree canopies changes over time and during the growing season, which can affect the accuracy of the model's estimates. This trend is typical in sparse crops at the beginning of the development growth stages in Mediterranean areas, where the weed cover growing in the inter-row area, resulting from the initial soil water content contaminates the pixel information [32,36]. Then, the inter-row weed cover dried naturally when the local conditions became hot and dry in early December (Fig. 2). This orchard characteristics affect the partitioning of the surface energy balance computed by the METRIC model and impacts the estimated ETa values in the orchard. The distribution of the canopy and bare soil has been shown to influence the determination of Kc, as has been extensively studied in the literature [38,60]. Furthermore, precipitation events can significantly influence soil evaporation rates, thereby affecting the METRIC model's computation process [26]. In such scenarios, it is often required to adjust the model to accurately reflect the impact of rainfall events, particularly in sparce crops. In this study, the lack of rain during the apple trees' growing season (Fig. 2) made it unnecessary to adjust the satellite-based ETa estimations [17]. These weather conditions are typical of Chile's Central Valley, which corresponds to a Mediterranean-type climatic conditions and with a decreasing rainfall trend in the last decade [6,61].

Indeed, the results obtained for the studied apple orchard can be considered with acceptable accuracy when Kc was computed on sparse crops (less than 20 %) [11,20]. The METRIC model and other Landsat-based single-layer models have a maximum resolution of 30×30 m (900 m^2), integrating canopy and soil elements at each pixel. However, when the thermal band is taken into account, this resolution is lower (60×60 m). Usually, the overall mean bias in similar estimated satellite-based ETa studies varied between 2 % and 25 % in different crops [11,20] found that the METRIC model had a MAE of 0.32 mm/day in estimating the overall ETa in the California plains. They computed seasonal adjusted Kc_{metric} values for apple trees between 0.58 ± 0.22 and 1.18 ± 0.22 for the growing season. The deviation levels of this study are consistent to those reported in the literature when single-layer satellite-based models were used to estimate the Kc and daily ETa. Also, similar studies on sparse crops, such as 'Merlot' vineyards, [56] found that the calibrated METRIC model overestimated the Kc by about 10 % with an RMSE and MAE of 0.10 and 0.08, respectively. The daily ETa values were also overestimated by 9 % (MAE = 0.50 mm/day and RMSE = 0.62 mm/day). In a study of super-intensive olive orchard, [34] adjusted the METRIC model-specific functions of LAI, Z_{om}, and surface temperature. This evaluation resulted in an overestimation of daily ETa by 11 %, with mean differences between EC measurements and METRIC-modeled ETa of 0.52 mm/day. Similarly, after adapting the calibrate METRIC functions of LAI, Z_{om}, and G to the drip-irrigated super-intensive olive orchard, [40] overestimated ETa by 6 %, compared to EC measurements. In Pistachio, [62] found that calibrations on Z_{om} directly impacted the daily ETa_{metric} estimations, resulting in an MAE and RMSE of 1.1 mm/day and 1.4 mm/day, respectively. Consistently with the findings of previous studies, the results of this study demonstrate the significant potential of remote sensing techniques to improve irrigation efficiency at various field scales [42,63,64].

4.2. Seasonal progression of satellite-based Kc across apple phenological stages

The higher differences in the Kc values estimated by the standard METRIC model could be attributed to the changes in the irrigation frequency, which varied from 2 to 5 days (data non show). These variations in the irrigation scheduling were most pronounced at the end of the growing season due to water supply restrictions imposed by the Chilean government due to the drought (Figs. 4 and 5 – DOY 62–78). The changes in the irrigation frequency and the severe drought conditions in the bare soil could have created imbalances in the G fluxes. The standard METRIC functions were unable to detect these imbalances, as they were developed for fully covered annual crops. Also, the Ψx values presented in Fig. 4 support the conclusion that the drip-irrigated apple orchard was well-watered throughout the growing season [65,66].

The METRIC model computes ETa as a residual of the surface energy balance, it means that any errors in the intermediate calculations of the RSEB can be propagated to the estimates of Kc and then ETa. Ref. [62] found that this can result in overestimating Kc_{metric} values. However, when calibrated functions were applied, the differences between the estimated and measured Kc values were minimized, with an average of 0.73 ± 0.07 for the same period. It is well known that the soil-vegetation-atmosphere water fluxes in woody canopies (with spacing between rows) are more complex than those observed in annual crops with full soil coverage [60,67]. In this context, the application of the specific calibration in the sub-models of METRIC for LAI, G, and Z_{om}, proposed by Ref. [33] (Table 3), was positive in reducing the bias in the estimation of Kc and ETa values in the studied apple orchard. Similar performance improvements have been reported in applying a calibrated version of the METRIC model for other sparse crops [32,34,41,62,68].

The highest differences in the Kc's values were observed for those suggested in the FAO-56 manual compared to the EC and METRIC outputs. Fig. 4 shows that single Kc estimated by the METRIC model and measurements from the EC system were substantially less than those suggested in the literature for apple trees at the initial, medium, and end growth stages. Differences in field management, cultivar, and planting spacing, among others, have been identified as sources of variability in Kc values. It highlights the need for adjusting Kc values proposed by the literature [11]. Both the standard and calibrated METRIC models depict the seasonal fluctuations of Kc during the crop season, following a Kc trend similar to that of the EC measured at ground level. The calibrated METRIC model seemed to track the seasonal variations of Kc in the drip-irrigated apple trees orchard better than the standard METRIC model. It is important to note that [69] reported similar Kc values (to those obtained in this study) in a 'pink lady' apple orchard using an EC system in South Africa, which has a Mediterranean-type climate. This study was corroborated by the results of [37], who reported similar Kc values on a 10-year-old apple trees using the weighing lysimeter technique.

4.3. Spatial-temporal patterns of crop coefficients and applications

The maps produced in this study provide a potential way to use remote sensing-based Kc to map the site-specific variability of apple trees' water consumption during the growing season. The irrigation management at the field scale, based on mid-resolution satellite images such as those obtained from Landsat products, has been suggested as a reliable alternative to the current Kc from the literature, which does not reflect the natural spatial variability of the field [70,71]. Also, [43] demonstrate the potential use of the calibrated METRIC model (LAI and Z_{om}) to compute ETa on a vineyard using high-resolution images from an unmanned aerial vehicle.

Efficient water resource management is increasingly evident in regions undergoing prolonged water stress. Over the recent decade, Mediterranean-type areas (such as Central Chile) have consistently experienced extended periods of drought, as documented by Refs. [6,7]. Such water constraints pose significant challenges for agricultural management, given the essential role of irrigation in crop yield optimization. Exploring new strategies for irrigation water management based on calibrated satellite models is not merely an operational consideration. It becomes a new factor in ensuring agricultural resilience and long-term sustainability over large areas. Considering the current climate change phenomenon, the higher dry and heat weather conditions increase the plant's water consumption [72], affecting the irrigation schedule. Thus, adjusting the Kc of different plots inside the field, considering their spatial variability estimated from the METRIC products (for each specific phenological stage), could positively impact water productivity, increasing production compared to the amount of water irrigated (water use efficiency, WUE).

Regulated deficit irrigation (RDI) presents a water-saving strategy with significant potential for apple orchards. When combined with calibrated remote sensing-based monitoring of ETa, this approach can optimize WUE and even improve fruit size and quality on a plot-by-plot basis [1,66,73]. In this context, the METRIC model, incorporating calibrated sub-models for LAI, Z_{om}, and G (as detailed in Table 3), emerges as a powerful decision-making tool for site-specific irrigation water management. Plot-specific adjustments based on real-time ETa data can optimize irrigation practices on apple orchards.

5. Conclusions

The calibrated METRIC model, incorporating functions of LAI, Z_{om}, and G overpredicted Kc and ETa values for a drip-irrigated apple orchard with errors less than 10 %, while the standard METRIC overpredicted Kc and ETa with errors of 18 % and 17 %, respectively. The observed discrepancies between standard METRIC estimates and measured values can be attributed to the dynamic ground cover between tree rows, particularly during early growth stages. Fluctuating weed cover, influenced by initial soil moisture, can distort remote sensing data. Furthermore, varying irrigation frequencies present additional challenges to the standard model's accuracy in Kc estimation. These findings highlight the limitations of the standard METRIC model in complex orchard ecosystems. In contrast, the calibrated METRIC model's ability to account for spatial variability through sub-models for LAI, Z_{om}, and G presents a significant advancement. This calibrated model offers a promising tool for irrigation management in apple orchards, particularly in Mediterranean climates facing water scarcity. By providing spatially Kc and ETa data, the calibrated METRIC model has the potential

to optimize irrigation scheduling, ensuring efficient water use and promoting sustainable orchard management.

CRediT authorship contribution statement

Daniel de la Fuente-Saiz: Writing – original draft, Validation. **Samuel Ortega-Farias:** Writing – original draft. **Marcos Carrasco-Benavides:** Writing – review & editing. **Samuel Ortega-Salazar:** Data curation. **Fei Tian:** Writing – review & editing. **Sufen Wang:** Writing – review & editing. **Yi Liu:**Writing – review & editing.

Declaration of competing interest

The authors declare that they have no known competing financial interests or personal relationships that could have appeared to influence the work reported in this paper.

Acknowledgements

This research was funded by the International and regional cooperation and exchange projects of the National Natural Science Foundation of China (51961125205) and the Chilean government through National Agency for Research and Development (ANID) (NSFC190013 and FSEQ210004) and ANID-Becas Doctorado Nacional (21182053).

References

[1] E. Atay, X. Crété, D. Loubet, P.E. Lauri, Diurnal and seasonal growth responses of apple trees to water-deficit stress, Erwerbsobstbau 65 (1) (2023) 1–6.
[2] F. Zhang, T. Wang, X. Wang, X. Lü, Apple pomace as a potential valuable resource for full-components utilization: a review, J. Clean. Prod. 329 (2021) 129676.
[3] A. AghaKouchak, D. Feldman, M. Hoerling, T. Huxman, J. Lund, Water and climate: recognize anthropogenic drought, Nat. News 524 (7566) (2015) 409.
[4] D. Badiu, F.H. Arion, I.C. Muresan, R. Lile, V. Mitre, Evaluation of economic efficiency of apple orchard investments, Sustainability 7 (8) (2015) 10521–10533.
[5] A. del Pozo, N. Brunel-Saldias, A. Engler, S. Ortega-Farias, C. Acevedo-Opazo, G.A. Lobos, M.A. Molina-Montenegro, Climate change impacts and adaptation strategies of agriculture in Mediterranean-climate regions (MCRs), Sustainability 11 (10) (2019) 2769.
[6] R.D. Garreaud, J.P. Boisier, R. Rondanelli, A. Montecinos, H.H. Sepúlveda, D. Veloso-Aguila, The Central Chile mega drought (2010–2018): a climate dynamics perspective, Int. J. Climatol. 40 (2020) 421–439, https://doi.org/10.1002/joc.6219.
[7] D. Urdiales, F. Meza, J. Gironás, H. Gilabert, Improving stochastic modelling of daily rainfall using the ENSO index: model development and application in Chile, Water 10 (2) (2018) 145.
[8] G. Boulet, L. Jarlan, A. Olioso, H. Nieto, Evapotranspiration in the mediterranean region, in: Water Resources in the Mediterranean Region, Elsevier, 2020, pp. 23–49.
[9] Z. Wang, G. Li, H. Sun, L. Ma, Y. Guo, Z. Zhao, L. Mei, Effects of drought stress on photosynthesis and photosynthetic electron transport chain in young apple tree leaves, Biol. Open 7 (11) (2018).
[10] R.G. Allen, L.S. Pereira, D. Raes, M. Smith, Crop Evapotranspiration. Guidelines for Computing Crop Water Requirements, Vol 56. FAO Irrigation and Drainage Paper (FAO), Italy, United Nations FAO, 1998.
[11] M. Mhawej, A. Nasrallah, Y. Abunnasr, A. Fadel, G. Faour, Better irrigation management using the satellite-based adjusted single crop coefficient (aKc) for over sixty crop types in California, USA, Agric. Water Manag. 256 (2021) 107059, https://doi.org/10.1016/j.agwat.2021.107059.
[12] D. Zanotelli, L. Montagnani, C. Andreotti, M. Tagliavini, Evapotranspiration and crop coefficient patterns of an apple orchard in a sub-humid environment, Agric. Water Manag. 226 (2019) 105756.
[13] R.G. Allen, L.S. Pereira, Estimating crop coefficients from fraction of ground cover and height, Irrigat. Sci. 28 (1) (2009) 17–34, https://doi.org/10.1007/s00271-009-0182-z.
[14] I.A. El-Magd, T. Tanton, Remote sensing and GIS for estimation of irrigation crop water demand, Int. J. Rem. Sens. 26 (11) (2005) 2359–2370, https://doi.org/10.1080/0143116042000298261.
[15] J. Girona, J. del Campo, M. Mata, G. Lopez, J. Marsal, A comparative study of apple and pear tree water consumption measured with two weighing lysimeters, Irrigat. Sci. 29 (1) (2011) 55–63, https://doi.org/10.1007/s00271-010-0217-5.
[16] S. Er-Raki, J.C. Rodriguez, J. Garatuza-Payan, C.J. Watts, A. Chehbouni, Determination of crop evapotranspiration of table grapes in a semi-arid region of Northwest Mexico using multi-spectral vegetation index, Agric. Water Manag. 122 (2013) 12–19, 84.
[17] M. Tasumi, R.G. Allen, R. Trezza, J.L. Wright, Satellite-based energy balance to assess within-population variance of crop coefficient curves, J. Irrigat. Drain. Eng. 131 (1) (2005) 94–109, https://doi.org/10.1061/(ASCE)0733-9437(2005)131:1(94).
[18] S.H. Mahmoud, T.Y. Gan, Irrigation water management in arid regions of Middle East: assessing spatio-temporal variation of actual evapotranspiration through remote sensing techniques and meteorological data, Agric. Water Manag. 212 (2019) 35–47.
[19] R.R. McShane, K.P. Driscoll, R. Sando, A review of surface energy balance models for estimating actual evapotranspiration with remote sensing at high spatiotemporal resolution over large extents. Scientific Investigations Report 2017–5087, US Geological Survey, Reston, VA, 2017, p. 19.
[20] K. Zhang, J.S. Kimball, S.W. Running, A review of remote sensing based actual evapotranspiration estimation, Wiley Interdiscipl. Rev.: Water 3 (6) (2016) 834–853.
[21] G. Olmedo, S. Ortega-Farías, D. De la Fuente-Sáiz, D. Fonseca-Luengo, F. Fuentes-Peñailillo, Water: tools and functions to estimate actual evapotranspiration using land surface energy balance models in R, R J. 8 (2) (2016) 352–369.
[22] J.M. Ramírez-Cuesta, R.G. Allen, D.S. Intrigliolo, A. Kilic, C.W. Robison, R. Trezza, I.J. Lorite, METRIC-GIS: an advanced energy balance model for computing crop evapotranspiration in a GIS environment, Environ. Model. Software (2020) 104770.
[23] F.S. Melton, J. Huntington, R. Grimm, J. Herring, M. Hall, D. Rollison, T. Erickson, et al., OpenET: filling a critical data gap in water management for the western United States, J. Am. Water Resour. Assoc. 58 (6) (2022) 971–994.
[24] W.G.M. Bastiaanssen, M. Menenti, R.A. Feddes, A.A.M. Holtslag, A remote sensing surface energy balance algorithm for land (SEBAL). 1. Formulation.", J. Hydrol. 212–213 (December) (1998) 198–212, https://doi.org/10.1016/S0022-1694(98)00253-4.
[25] M. Mhawej, G. Faour, Open-source Google Earth Engine 30-m evapotranspiration rates retrieval: the SEBALIGEE system, Environ. Model. Software 133 (2020) 104845, https://doi.org/10.1016/j.envsoft.2020.104845.
[26] R.G. Allen, M. Tasumi, R. Trezza, Satellite-based energy balance for mapping evapotranspiration with internalized calibration (METRIC)—model, J. Irrigat. Drain. Eng. 133 (4) (2007) 380–394.
[27] G.J. Roerink, Z. Su, M. Menenti, S-SEBI: a simple remote sensing algorithm to estimate the surface energy balance, Phys. Chem. Earth - Part B Hydrol., Oceans Atmos. 25 (2) (2000) 147–157, https://doi.org/10.1016/S1464-1909(99)00128-8.

[28] J.M. Norman, W.P. Kustas, K.S. Humes, Source approach for estimating soil and vegetation energy fluxes in observations of directional radiometric surface temperature, Agric. Forest Meteorol. Therm. Remote Sens. Energy Water Balance Over Vegetation 77 (3) (1995) 263–293, https://doi.org/10.1016/0168-1923(95)02265-Y.

[29] A. Mokhtari, H. Noory, M. Vazifedoust, M. Bahrami, Estimating net irrigation requirement of winter wheat using model-and satellite-based single and basal crop coefficients, Agric. Water Manag. 208 (2018) 95–106.

[30] A. Mokhtari, H. Noory, F. Pourshakouri, P. Haghighatmehr, Y. Afrasiabian, M. Razavi, A.S. Naeni, Calculating potential evapotranspiration and single crop coefficient based on energy balance equation using Landsat 8 and Sentinel-2, ISPRS J. Photogrammetry Remote Sens. 154 (2019) 231–245.

[31] G. Petropoulos, Remote sensing of surface turbulent energy fluxes, in: Remote Sensing of Energy Fluxes and Soil Moisture Content, by George Petropoulos, CRC Press, 2013, pp. 49–84. http://www.crcnetbase.com/doi/abs/10.1201/b15610-5.

[32] M. Carrasco-Benavides, S. Ortega-Farías, L. Lagos, J. Kleissl, L. Morales-Salinas, A. Kilic, Parameterization of the satellite-based model (METRIC) for the estimation of instantaneous surface energy balance components over a drip-Irrigated vineyard, Remote Sens. 2014 6 (2014) 11342–11371.

[33] D. de la Fuente-Sáiz, S. Ortega-Farías, D. Fonseca, S. Ortega-Salazar, A. Kilic, R. Allen, Calibration of metric model to estimate energy balance over a drip-irrigated apple orchard, Rem. Sens. 9 (7) (2017) 670.

[34] I. Póças, T.A. Paço, M. Cunha, J.A. Andrade, J. Silvestre, A. Sousa, R.G. Allen, Satellite-based evapotranspiration of a super-intensive olive orchard: application of METRIC algorithms, Biosyst. Eng. 128 (2014) 69–81.

[35] S. Ortega-Farías, D. Fonseca, D. de la Fuente, A. Kilic, S. Ortega-Salazar, R. Allen, M. Carrasco-Benavides, Remote sensing model to evaluate the spatial variability of vineyard water requirements, in: X International Symposium on Grapevine Physiology and Biotechnology, 2016, pp. 235–242, 1188.

[36] J.M. Ramírez-Cuesta, R.G. Allen, P.J. Zarco-Tejada, A. Kilic, C. Santos, I.J. Lorite, Impact of the spatial resolution on the energy balance components on an open-canopy olive orchard, Int. J. Appl. Earth Obs. Geoinf. 74 (2019) 88–102.

[37] J. Marsal, J. Girona, J. Casadesus, G. Lopez, C.O. Stöckle, Crop coefficient (Kc) for apple: comparison between measurements by a weighing lysimeter and prediction by CropSyst, Irrigat. Sci. 31 (3) (2013) 455–463.

[38] R. López-Olivari, S. Ortega-Farías, C. Poblete-Echeverría, Partitioning of net radiation and evapotranspiration over a super-intensive drip-irrigated olive orchard. Irrigation science, 1, in: J. Payero, C. Neale, J. Wright (Eds.), 2005. Estimating Soil Heat Flux for Alfalfa and Clipped Tall Fescue Grass, vol. 34, 2016, pp. 17–31. Am. Soc. Agric. Eng. 2005, 21, 401–409.

[39] M. Carrasco-Benavides, S. Ortega-Farías, P.M. Gil, D. Knopp, L. Morales-Salinas, L.O. Lagos, S. Fuentes, Assessment of the vineyard water footprint by using ancillary data and EEFlux satellite images. Examples in the Chilean central zone, Sci. Total Environ. 811 (2022) 152452.

[40] S. Ortega-Salazar, S. Ortega-Farías, A. Kilic, R. Allen, Performance of the METRIC model for mapping energy balance components and actual evapotranspiration over a superintensive drip-irrigated olive orchard, Agric. Water Manag. 251 (2021) 106861.

[41] C. Santos, I.J. Lorite, R.G. Allen, M. Tasumi, Aerodynamic parameterization of the satellite-based energy balance (METRIC) model for ET estimation in rainfed olive orchards of Andalusia, Spain, Water Resour. Manag. 26 (11) (2012) 3267–3283.

[42] M. González-Dugo, J. Gonzalez-Piqueras, I. Campos, C. Balbontin, A. Calera, Estimation of surface energy fluxes in vineyard using field measurements of canopy and soil temperature, Remote Sens. Hydrol. 352 (2012) 59–62.

[43] J.M. Ramírez-Cuesta, D.S. Intrigliolo, I.J. Lorite, M.A. Moreno, D. Vanella, R. Ballesteros, I. Buesa, Determining grapevine water use under different sustainable agronomic practices using METRIC-UAV surface energy balance model, Agric. Water Manag. 281 (2023) 108247.

[44] S. Musacchi, I. Iglesias, D. Neri, Training systems and sustainable orchard management for European pear (Pyrus communis L.) in the Mediterranean area: a review, Agronomy 11 (9) (2021) 1765.

[45] P. Romero, J.M. Navarro, P.B. Ordaz, Towards a sustainable viticulture: the combination of deficit irrigation strategies and agroecological practices in Mediterranean vineyards. A review and update, Agric. Water Manag. 259 (2022) 107216.

[46] M. Zambrano-Bigiarini, O.M. Baez-Villaneuva, Characterizing meteorological droughts in data scare regions using remote sensing estimates of precipitation, in: Extreme Hydroclimatic Events and Multivariate Hazards in a Changing Environment, Elsevier, 2019, pp. 221–246.

[47] U. Meier, Growth stages of mono- and dicotyledonous plants, BBCH Monograph (2001), https://doi.org/10.5073/bbch0515. Archived from the original on 2018-10-15.

[48] C. Poblete-Echeverría, S. Ortega-Farias, Evaluation of single and dual crop coefficients over a drip-irrigated Merlot vineyard (Vitis vinifera L.) using combined measurements of sap flow sensors and eddy covariance system, Aust. J. Vitic. 2013 19 (2013) 249–260.

[49] R.G. Allen, I.A. Walter, R.L. Elliott, T.A. Howell, D. Itenfisu, M.E. Jensen, R.L. Snyder, The ASCE Standardized Reference Evapotranspiration Equation, 2005.

[50] K.R. Thorp, pyfao56: FAO-56 evapotranspiration in Python, SoftwareX 19 (2022) 101208.

[51] J. Laubach, M. Raschendorfer, H. Kreilein, G. Gravenhorst, Determination of heat and water vapour fluxes above a spruce forest by eddy correlation, Agric. For. Meteorol. 71 (1994) 373–401.

[52] S. Li, S. Kang, F. Li, L. Zhang, B. Zhang, Vineyard evaporative fraction based on eddy covariance in an arid desert region of northwest China, Agric. Water Manag. 95 (2008) 937–948.

[53] C. Poblete-Echeverría, S. Ortega-Farias, Estimation of actual evapotranspiration for a drip-irrigated merlot vineyard using a three-source model, Irrigat. Sci. 28 (2009) 65–78.

[54] T.E. Twine, W.P. Kustas, J.M. Norman, D.R. Cook, P.R. Houser, T.P. Meyers, J.H. Prueger, P.J. Starks, M.L. Wesely, Correcting eddy covariance flux underestimates over a grassland, Agric. For. Meteorol. 103 (2000) 279–300.

[55] J. Payero, C. Neale, J. Wright, Estimating soil heat flux for alfalfa and clipped tall fescue grass, Am. Soc. Agric. Eng. 21 (2005) 401–409.

[56] M. Carrasco-Benavides, S. Ortega-Farías, L.O. Lagos, J. Kleissl, L. Morales, C. Poblete-Echeverría, R.G. Allen, Crop coefficients and actual evapotranspiration of a drip-irrigated merlot vineyard using multispectral satellite images, Irrigat. Sci. 30 (6) (2012) 485–497, https://doi.org/10.1007/s00271-012-0379-4.

[57] Q. Chen, L. Jia, R. Hutjes, M. Menenti, Estimation of aerodynamic roughness length over oasis in the Heihe river basin by utilizing remote sensing and ground data, Remote Sens. 7 (2015) 3690–3709.

[58] C. Willmott, Some comments on the evaluation of model performance, Bull. Am. Meteorol. Soc. 63 (1982) 1309–1313.

[59] R. Tang, Z.-L. Li, X. Sun, Temporal upscaling of instantaneous evapotranspiration: an intercomparison of four methods using eddy covariance measurements and MODIS data, Remote Sens. Environ. 2013 138 (2013) 102–118.

[60] T. Kato, M. Kamichika, Determination of a crop coefficient for evapotranspiration in a sparse sorghum field, Irrigat. Drain.: J. Int. Comm. Irrig. Drainage 55 (2) (2006) 165–175.

[61] M.J. Deitch, M.J. Sapundjieff, S.T. Feirer, Characterizing precipitation variability and trends in the world's Mediterranean-climate areas, Water 9 (4) (2017) 259.

[62] Y. Jin, R. He, G. Marino, M. Whiting, E. Kent, B.L. Sanden, M. Culumber, L. Fergusom, C. Little, S. Grattan, K. Tha Paw U, L.O. Lagos, R. Snyder, D. Zaccaria, Spatially variable evapotranspiration over salt affected pistachio orchards analyzed with satellite remote sensing estimates, Agric. For. Meteorol. 262 (2018) (2018) 178–191. ISSN 0168-192.

[63] H. Büyükcangaz, D.D. Steele, S.R. Tuscherer, D.G. Hopkins, X. Jia, Evapotranspiration mapping with METRIC to evaluate effectiveness of irrigation in flood mitigation for the Devils Lake Basin, Trans. ASABE 60 (5) (2017) 1575–1591.

[64] A. Reyes-González, J. Kjaersgaard, T. Trooien, C. Hay, L. Ahiablame, Comparative Analysis of METRIC model and atmometer methods for estimating actual evapotranspiration, Int. J. Agron. 2017 (2017).

[65] S. Espinoza-Meza, S. Ortega-Farias, R. López-Olivari, M. Araya-Alman, M. Carrasco-Benavides, Response of fruit yield, fruit quality, and water productivity to different irrigation levels for a microsprinkler-irrigated apple orchard (cv. Fuji) growing under Mediterranean conditions, Eur. J. Agron. 145 (2023) 126786, https://doi.org/10.1016/j.eja.2023.126786.

[66] M.G. O'Connell, I. Goodwin, Responses of "pink lady" apple to deficit irrigation and partial rootzone drying: physiology, growth, yield, and fruit quality, Aust. J. Agric. Res. 58 (2007) 1068–1076.

[67] T. Kato, R. Kimura, M. Kamichika, Estimation of evapotranspiration, transpiration ratio and water-use efficiency from a sparse canopy using a compartment model, Agric. Water Manag. 65 (3) (2004) 173–191.
[68] R. He, Y. Jin, M. Kandelous, D. Zaccaria, B. Sanden, R. Snyder, J. Hopmans, Evapotranspiration estimate over an almond orchard using landsat satellite observations, Rem. Sens. 9 (5) (2017) 436.
[69] M. Gush, S. Dzikiti, M. van Der Laan, M. Steyn, S. Manamathela, H. Pienaar, Field quantification of the water footprint of an apple orchard, and extrapolation to watershed scale within a winter rainfall Mediterranean climate zone, Agric. For. Meteorol. 271 (2019) 135–147.
[70] S.O. Ihuoma, C.A. Madramootoo, M. Kalacska, Integration of satellite imagery and in situ soil moisture data for estimating irrigation water requirements, Int. J. Appl. Earth Obs. Geoinf. 102 (2021) 102396.
[71] T. Wiederstein, V. Sharda, J. Aguilar, T. Hefley, I.A. Ciampitti, A. Sharda, K. Igwe, Evaluating spatial and temporal variations in sub-field level crop water demands, Front. Agron. 4 (2022) 983244.
[72] J.L. Hatfield, C. Dold, Water-use efficiency: advances and challenges in a changing climate, Front. Plant Sci. 10 (2019).
[73] S. Faghih, Z. Zamani, R. Fatahi, A. Liaghat, Effects of deficit irrigation and kaolin application on vegetative growth and fruit traits of two early ripening apple cultivars, Biol. Res. 52 (2019).